UNIVERSITY OF BIRMINGHAM
University of Birmingham Research at Birmingham

A microstrip lossy diplexer with flat channel passbands

Zhang, Fan; Wu, Yun; Sun, Liang; Gao, Yang; Wang, Yi; Xu, Jun

DOI:
10.2528/PIERM20011605

License:
None: All rights reserved

Document Version
Peer reviewed version

Citation for published version (Harvard):
Zhang, F, Wu, Y, Sun, L, Gao, Y, Wang, Y & Xu, J 2020, 'A microstrip lossy diplexer with flat channel passbands', *Progress In Electromagnetics Research M*, vol. 90, pp. 99-108.
https://doi.org/10.2528/PIERM20011605

Link to publication on Research at Birmingham portal

General rights
Unless a licence is specified above, all rights (including copyright and moral rights) in this document are retained by the authors and/or the copyright holders. The express permission of the copyright holder must be obtained for any use of this material other than for purposes permitted by law.

•Users may freely distribute the URL that is used to identify this publication.
•Users may download and/or print one copy of the publication from the University of Birmingham research portal for the purpose of private study or non-commercial research.
•User may use extracts from the document in line with the concept of 'fair dealing' under the Copyright, Designs and Patents Act 1988 (?)
•Users may not further distribute the material nor use it for the purposes of commercial gain.

Where a licence is displayed above, please note the terms and conditions of the licence govern your use of this document.

When citing, please reference the published version.

Take down policy
While the University of Birmingham exercises care and attention in making items available there are rare occasions when an item has been uploaded in error or has been deemed to be commercially or otherwise sensitive.

If you believe that this is the case for this document, please contact UBIRA@lists.bham.ac.uk providing details and we will remove access to the work immediately and investigate.

Download date: 04. May. 2023

Machine Copy for Proofreading, Vol. x, y–z, 2020

A Microstrip Lossy Diplexer with Flat Channel Passbands

Fan Zhang[1], Yun Wu[2], Liang Sun[2], Yang Gao[3], Yi Wang[4, *], and Jun Xu[1]

Abstract—Passband flatness and band-edge selectivity in microwave filters with finite quality-factor resonators can be improved by the synthesis of lossy filters. This paper demonstrates the extension of this technique to a lossy diplexer by means of resistive coupling. A dual-mode stub-loaded resonator (SLR) junction and a fork-like feedline are used in the diplexer to address the challenge of independently controlling the external coupling from the common port to the two channel filters and therefore enable flexible realization of the channel bandwidth. The coupling matrices with resistive couplings for the lossy diplexer are generated. For verification, a microstrip lossy diplexer operating at 1.91 and 2.6 GHz was designed and tested. The flatness of the passband has been significantly improved, with a reduction of the passband insertion loss variation from 1.4/1.2 dB to 0.66/0.63 dB for the low/high band. The measured results are in good agreement with the simulations as well as the theoretical responses from the coupling matrix. This was also experimentally compared with a reference diplexer without resistive couplings.

1. INTRODUCTION

Loss has a major impact on the synthesis and realization of filters. Traditional filter synthesis assumes lossless resonators of an infinite quality factor (Q-factor). When applied to practical resonators of relatively low Q-factor, the frequency responses suffer from a degradation of performance in terms of insertion loss and selectivity especially at the bend edges, which affects the flatness of the insertion loss over the passband [1–11]. This particularly concerns narrowband filters where the variation of the insertion loss over the passband increases and puts extra burden on power equalization from the system design point of view. This adverse impact can be alleviated by the 'lossy filter' technique, which can restore in-band flatness and sharp transition (high selectivity) at the cost of increased insertion loss. Fortunately, this additional insertion loss can be readily compensated for by amplification in many applications. It is worth noting that 'lossy filter' is an established terminology to describe the type of filters that achieve flatter insertion loss over the passband using resonators with ununiform quality factors [12, 13] or by deliberately introducing lossy elements such as coupling resistors [14, 15]. This terminology has been used to distinguish from conventional filters with inherent finite quality factors (and therefore losses) without any extra resistive elements. So far, the lossy filter technique has only been applied to fix-band two-port filters. There is a demand from some niche applications to extend this technique to diplexers and multiplexers. As an example, for the C-band input multiplexers (IMUXs) in satellites, being able to use compact low-Q microstrip resonators while maintaining the pass-band flatness and selectivity will significantly reduce their size and mass. This is highly desirable for space applications.

This paper reports our work towards this direction. To the best knowledge of the authors, this is the first demonstrated 'lossy diplexer' in open literature, where dissipative cross couplings are used.

Received 16 January 2020

* Corresponding author: Yi Wang (y.wang.1@bham.ac.uk).

[1] School of Physics, University of Electronic Science and Technology of China, Chengdu 610054, China. [2] National Laboratory for Superconductivity, Institute of Physics, Chinese Academy of Sciences, Beijing, China. [3] Department of Information Engineering, Zhengzhou University, Zhengzhou 450001, China. [4] Department of Electronic, Electrical and Systems Engineering, University of Birmingham, Edgbaston, Birmingham B15 2TT, U.K..

We borrowed from the concept of 'lossy filter' and coined the terminology 'lossy diplexer'. To discern the difference between a lossy diplexer and a conventional diplexer, the latter will be described as a reference diplexer in this paper, which only has inherent losses without any added resistive elements.

In addition, instead of using a transmission-line based junction, two lossy filters are combined using a resonant junction formed of a dual-mode sub-loaded resonator (SLR). The junction contributes to a transmission pole for both the lower and the higher channels without adversely increasing the circuit size [16, 17], and therefore improving the selectivity of both channels. However, this all-resonator based diplexer structure increases the challenge in the design, where the SLR resonant junction, being part of both channel filters, would normally require to accommodate specific coupling to each of the two channels. To be able to independently control the coupling from the common port to the two channels via the SLR, a novel feeding structure, first reported in [18], was adopted here. This allows more flexible control of the channel bandwidth, which has significant benefit in real diplexer applications. This paper focuses on demonstrating the new device function of a lossy diplexer rather than the circuit layout innovation.

The main contribution of the paper is a new type of diplexer with flat channel passbands realized using a unique combination of technologies between lossy filters and all-resonator based diplexers with independently controllable channel bandwidth. The improved flatness of the passbands has been achieved by using resistive couplings. The synthesis of the coupling matrix and the design of the microstrip lossy diplexer are much more involved than those of conventional diplexers. This paper presents the design methodology and results with detailed comparisons.

The rest of the paper is organized as follows. The topologies of the all-resonator based lossy diplexer and a reference diplexer will be first introduced and their coupling matrices are obtained. This is followed by a brief discussion of the feeding structure that allows independent control of the coupling to the two channels, and the detailed designs of the reference and the lossy diplexer with simulation results. The measurement results will be given before the conclusion.

2. DIPLEXER TOPOLOGIES AND COUPLING MATRICES

Figure 1 shows the topologies of the reference diplexer and the lossy diplexer used in this work. They are formed of coupled resonators without any transmission line junctions. Each circle in the two channels denotes a resonator. The junction is a dual-mode sub-loaded resonator (SLR) with its two resonant modes (marked as '1' and '5' in Figure 1) corresponding to the respective central frequencies of the two channels. It forms one respective transmission pole for each channel filter.

The coupling topology of the lossy diplexer is depicted in Figure 1(b). The resistors R_i $(i = 1, 2, 3, 4)$ represent the resistance cross coupling between resonators. For each channel filter, a resistive cross coupling configuration similar to the one in [15] was used. This configuration is an effective and one of the simplest configurations to implement using microstrip resonators with uniform Q-factors. The latter point will be further elucidated by this work. For the lossy diplexer, one main design objective is to minimize the variation of the insertion loss in the passband.

For comparison, the diplexer of the same coupling topology but without the four resistive cross couplings is used as the reference design in Figure 1(a). Both the reference diplexer and the lossy diplexer are designed at 1.91 GHz (f_L) and 2.6 GHz (f_H) with the fractional bandwidth (FBW) of 4.6% and 6.5% respectively. The choice of frequencies is only for demonstration in this case. The return losses for the two channels are specified to be better than 20 dB. The diplexers are designed using half-wavelength hairpin resonators, and fabricated on a Rogers 4003C substrate with a thickness of 1.524 mm. The dielectric constant of the substrate is 3.55, and the loss tangent is 0.0029. The copper laminate is 18-µm thick. Using this substrate, the unloaded quality factors of the hairpin resonators are approximately 230 and 240 for the lower and higher channels, respectively, according to simulations. These Q values are considered in the coupling matrix to represent the loss. Since the two modes of the junction resonator are widely separated in frequency to tune with the two channels, the coupling matrices for the two channels can be obtained independently (assuming $m_{15} = 0$). For the reference diplexer, using a general coupling matrix synthesis method [19], the coupling matrices of the lower and higher channels can be expressed as

	1	2	3	4
1	−j0.094	0.911	0	0
2	0.911	−j0.094	0.700	0
3	0	0.700	−j0.094	0.911
4	0	0	0.911	−j0.094

	5	6	7	8
5	−j0.064	0.911	0	0
6	0.911	−j0.064	0.700	0
7	0	0.700	−j0.064	0.911
8	0	0	0.911	−j0.064

where the diagonal elements (j0.094 and j0.064) are utilized to model the finite quality factor (loss) of the resonators for the lower and higher channels. The normalized external quality factors for the three ports are 1.035.

For the lossy diplexer, the diagonal elements of the lossy diplexer matrix contain the loss contributions from both the resonator and the associated resistive coupling. Assuming the lower and higher channel filters are symmetrical, the resistive cross coupling coefficients are led to $m_{13} = m_{24}$, and $m_{57} = m_{68}$. The coupling matrix of the lower channel can be expressed as

	1	2	3	4
1	$-\text{j}0.094 - \lvert m_{13}\rvert$*j	0.911	$-m_{13}$*j	0
2	0.911	$-\text{j}0.094 - \lvert m_{13}\rvert$*j	0.700	$-m_{24}$*j
3	$-m_{13}$*j	0.700	$-\text{j}0.094 - \lvert m_{13}\rvert$*j	0.911
4	0	$-m_{24}$*j	0.911	$-\text{j}0.094 - \lvert m_{13}\rvert$*j

Similarly, the coupling matrix of the higher channel can be expressed as

	5	6	7	8
5	$-\text{j}0.064 - \lvert m_{57}\rvert$*j	0.911	$-m_{57}$*j	0
6	0.911	$-\text{j}0.064 - \lvert m_{57}\rvert$*j	0.700	$-m_{68}$*j
7	$-m_{57}$*j	0.700	$-\text{j}0.064 - \lvert m_{57}\rvert$*j	0.911
8	0	$-m_{68}$*j	0.911	$-\text{j}0.064 - \lvert m_{57}\rvert$*j

The resistive coupling coefficients m_{13} and m_{57} are obtained by using the approach from [15, 20], and they are optimized to be $m_{13} = 0.053$ and $m_{57} = 0.039$. Accordingly, the coupling matrices of the lower and higher channels can be given as

	1	2	3	4
1	−j0.147	0.911	−j0.053	0
2	0.911	−j0.147	0.700	−j0.053
3	−j0.053	0.700	−j0.147	0.911
4	0	−j0.053	0.911	−j0.147

	5	6	7	8
5	−j0.103	0.911	−j0.039	0
6	0.911	−j0.103	0.700	−j0.039
7	−j0.039	0.700	−j0.103	0.911
8	0	−j0.039	0.911	−j0.103

Its normalized external quality factors are identical with the reference diplexer.

Figure 2 compares the calculated S-parameter responses of these two diplexers from the matrices. One can see the lossy diplexer offers much improved flatness and sharper band-edges compared with the reference diplexer. For the reference one, the variation of insertion loss in the passband is around 1.3 dB (lower band) and 1.1 dB (higher band). The insertion losses are 1.63 and 1.47 dB, respectively. For the lossy diplexer, the variation of the insertion loss for the lower and higher channels is reduced to 0.6 dB. As a trade-off, the insertion losses increase to 3.8 and 2.9 dB.

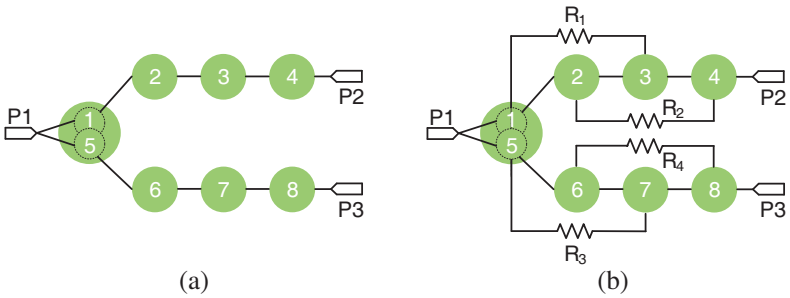

Figure 1. Topologies of the diplexers. (a) The reference diplexer. (b) The Lossy diplexer with resistive couplings.

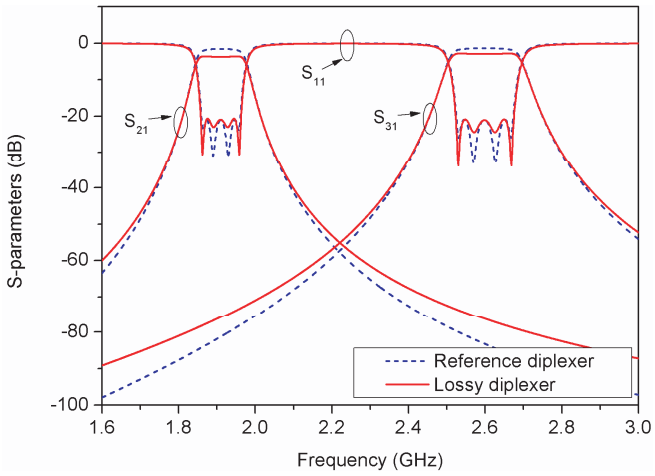

Figure 2. Calculated S-parameter response of the reference diplexer with finite Q-factor and the lossy diplexer from the coupling matrices.

3. DESIGN AND SIMULATIONS

3.1. Independently Controllable Coupling to the Resonant Diplexer Junction

As shown in Figure 3, the dual-mode junction resonator is implemented using a microstrip stub-loaded resonator. The rest are hairpin resonators. For the SLR [21], the line section l_{b10} is approximately the same as $l_{b6}+l_{b7}$. The open stub roughly has a length of $l_{stub}=l_{b8}-l_{b7}+l_{b9}$. Although it is not a strictly symmetric structure, it can be treated approximately using the odd-even mode analysis [21]. The odd mode frequency is determined by l_{b10} as

$$f_{odd}=\frac{c}{4l_{b10}\sqrt{\varepsilon_{eff}}} \tag{1}$$

where c is the light speed in free space and ε_{eff} is the effective permittivity of the microstrip substrate. Assuming the SLR has a uniform line width, the even mode resonant frequency is determined by the electrical lengths of the stub l_{stub} as well as l_{b10} as

$$\cot(\theta_{stub})\tan(\theta_{b10})=-2 \tag{2}$$

The SLR junction resonator resonates at 1.91 GHz (even mode) and 2.6 GHz (odd mode), corresponding to the central frequencies of the two channels respectively. The SLR resonator is folded into an upside-down Y-shape. The two modes can be clearly identified in the simulated current density distribution in Figures 4(a) and (b). The fork-liked feedline is used to independently control the coupling to the two channels. Each branch of the fork provides the edge coupling to one mode of the SLR. The folded longer branch is about half of the guided wavelength at 2.6 GHz. It presents an open circuit

and stops the higher channel signal from entering the lower channel, as can be seen from the simulated current distribution in Figure 4(b). The external coupling to the two channels can be individually tuned by adjusting the gap of g_1 or g_2 while keeping other dimensions fixed, as demonstrated previously in [18].

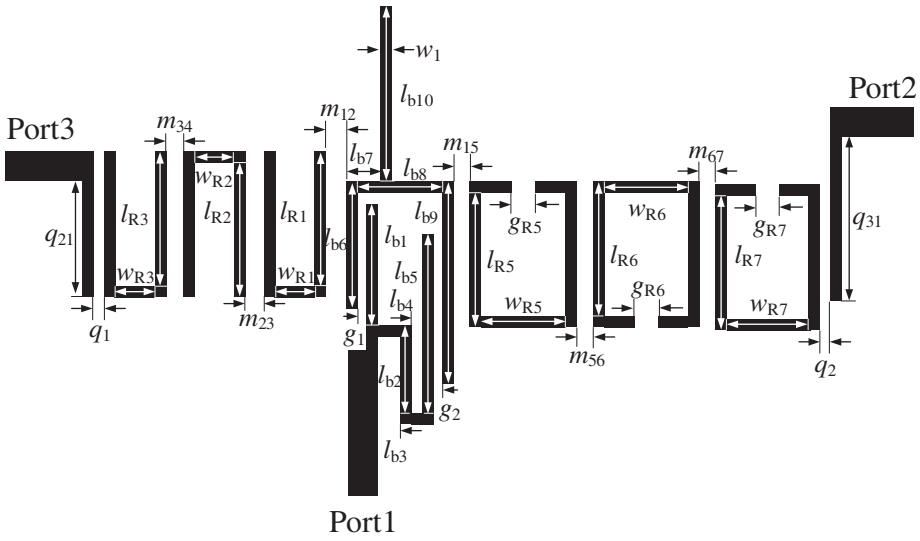

Figure 3. Layout of the referenced diplexer with the SLR at the junction and the external coupling structure at the common port which provides independently controllable coupling to the two channels ($l_{b1} = 15.86$, $l_{b2} = 10.94$, $l_{b3} = 2$, $l_{b4} = 0.88$, $l_{b5} = 25.54$, $l_{b6} = 14$, $l_{b7} = 2.9$, $l_{b8} = 7.5$, $l_{b9} = 23.8$, $l_{b10} = 19.64$, $l_{R1} = 15.8$, $l_{R2} = 15.7$, $l_{R3} = 15.8$, $l_{R5} = 14.75$, $l_{R6} = 14.65$, $l_{R7} = 14.3$, $w_{R1} = 4$, $w_{R2} = 4$, $w_{R3} = 4.04$, $w_{R5} = 9.6$, $w_{R6} = 9.6$, $w_{R7} = 9.44$, $g_{R5} = 2.3$, $g_{R6} = 2.26$, $g_{R7} = 2$, $m_{12} = 2.34$, $m_{23} = 2.6$, $m_{34} = 2.26$, $m_{15} = 2.52$, $m_{56} = 2.7$, $m_{67} = 2.4$, $q_1 = 0.9$, $q_2 = 0.7$, $q_{21} = 13.6$, $q_{31} = 18.64$, $w_1 = 1$, $g_1 = 0.76$, and $g_2 = 1.2$. units: mm).

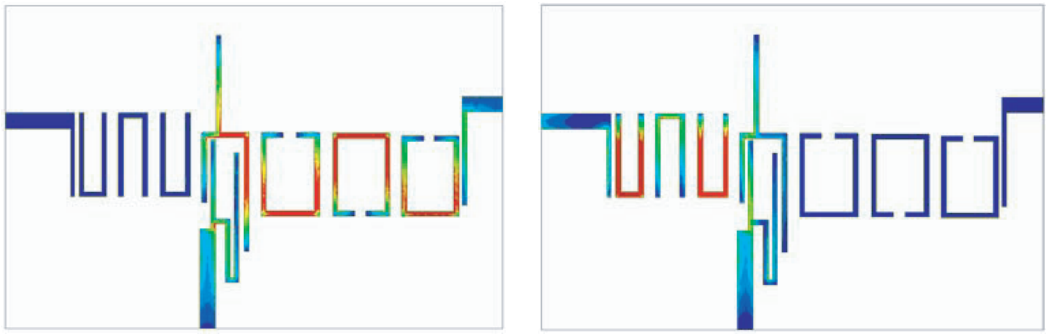

(a) (b)

Figure 4. Simulated current distribution at (a) 1.91 GHz and (b) 2.6 GHz of the reference diplexer.

3.2. Reference Diplexer

The reference diplexer and lossy diplexer were both designed to have a four-pole Chebyshev response at each channel based on the external coupling structure. The two diplexers have the same fractional bandwidths. Hairpin resonators with a line width of 1 mm were chosen for the construction of the diplexer. The initial lengths of the resonators for the lower and higher channels are half-wavelength at the center frequencies of the corresponding channels. The layout of the diplexer is shown in Figure 3.

The design process of the diplexer can be found in [18]. The optimized critical dimensions are given in the figure caption. The diplexer was simulated and optimized in Ansys EM simulator HFSS [22]. The simulated response of the diplexer is shown in Figure 5 in comparison with theoretical ones obtained from the coupling matrix. They are in good agreement with each other. It is noted that several transmission zeros are produced. These are attributed to the stubs of the fork-like feeding structure and the junction resonator of the diplexer, which cannot be accounted for by the coupling matrix. The isolation between the two channels are better than 50 dB.

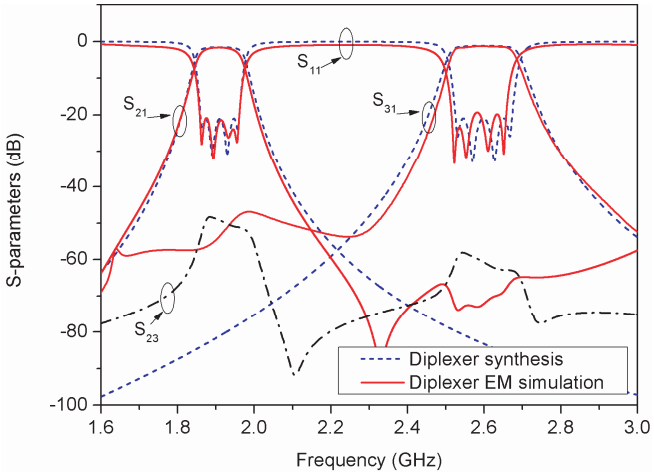

Figure 5. Reference diplexer EM simulation results in comparison with theoretical results based on the coupling matrix with finite Q-factor but without resistive couplings. The simulated isolation parameter (S_{23}) is shown in a black dash dot line.

3.3. Lossy Diplexer

The proposed lossy diplexer is implemented using microstrip structures, as shown in Figure 6. The channel filters and the coupling structure at the junction are similar to the reference diplexer. The resistive cross couplings are realized by surface mounted resistors placed between two sections of thin high-impedance lines, whose initial lengths are determined to be quarter of a wavelength at the respective channel center frequencies. The resistor value was first estimated from the resistive coupling, m_{res}, by [15]

$$R = \frac{1}{m_{res} b FBW} \tag{3}$$

where b is the susceptance slope of the resonator. The convenient rounded value of 300-Ω was chosen after optimization. The main dimensions of the diplexer after optimization are given in the caption of Figure 6.

The simulation results are compared to theoretical ones calculated from the coupling matrix as shown in Figure 7. Very good agreement has been achieved. As observed in Figure 5 and Figure 7, it can be seen that the resistive couplings do not adversely affect the isolation performance of the diplexer.

4. FABRICATION AND MEASUREMENT

Fabrication was made by a LPKF ProtoMat S63 micro milling machine. The overall dimension of both diplexers is 100 mm × 60 mm and the minimum gap used is 0.35 mm. The fabricated circuits are shown in Figure 8. Measurements were taken by an Agilent N5230A network analyzer. For the reference diplexer, as shown in Figure 9, the measured average insertion loss and its variation over the passband are 1.95 dB and 1.4 dB for the lower band, and 1.83 dB and 1.2 dB for the higher band. The small deviation between the simulated and measured results is believed to be mainly due to the tolerances of the fabrication.

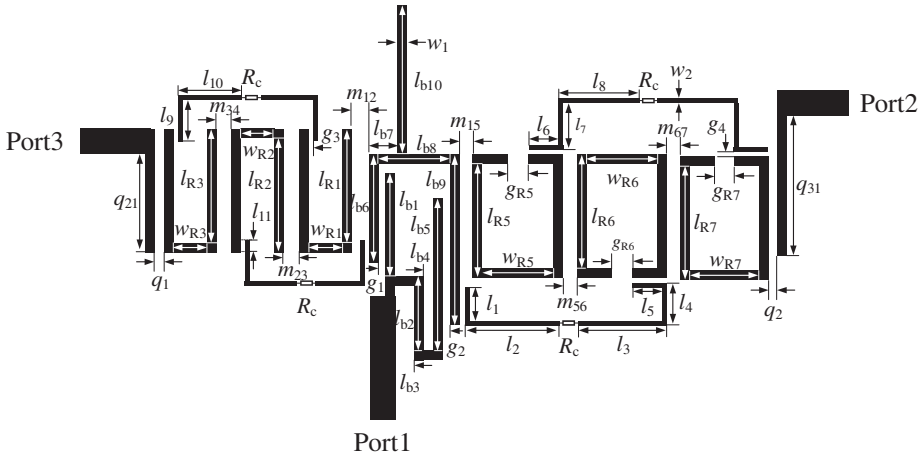

Figure 6. Layout of the lossy diplexer ($l_1 = 5.5$, $l_2 = 13.3$, $l_3 = 13.2$, $l_4 = 6.65$, $l_5 = 4.25$, $l_6 = 4.25$, $l_7 = 5.6$, $l_8 = 11$, $l_9 = 5.55$, $l_{10} = 7.35$, $l_{11} = 2.15$, $l_{b1} = 15.85$, $l_{b2} = 11.95$, $l_{b3} = 2$, $l_{b4} = 0.75$, $l_{b5} = 25.15$, $l_{b6} = 14$, $l_{b7} = 2.9$, $l_{b8} = 7.5$, $l_{b9} = 23.8$, $l_{b10} = 19.65$, $l_{R1} = 15.75$, $l_{R2} = 15.75$, $l_{R3} = 15.75$, $l_{R5} = 14.75$, $l_{R6} = 14.65$, $l_{R7} = 14.3$, $w_{R1} = 4$, $w_{R2} = 3.9$, $w_{R3} = 3.55$, $w_{R5} = 9.7$, $w_{R6} = 9.5$, $w_{R7} = 9.45$, $g_{R5} = 2.65$, $g_{R6} = 2.25$, $g_{R7} = 2.1$, $m_{12} = 2.3$, $m_{23} = 2.6$, $m_{34} = 2.35$, $m_{15} = 2.45$, $m_{56} = 2.65$, $m_{67} = 2.4$, $q_1 = 0.9$, $q_2 = 0.65$, $q_{21} = 13.6$, $q_{31} = 18.8$, $w_1 = 1$, $w_2 = 0.5$, $g_1 = 0.75$, $g_2 = 1$, $g_3 = 0.35$, and $g_4 = 0.45$. units: mm).

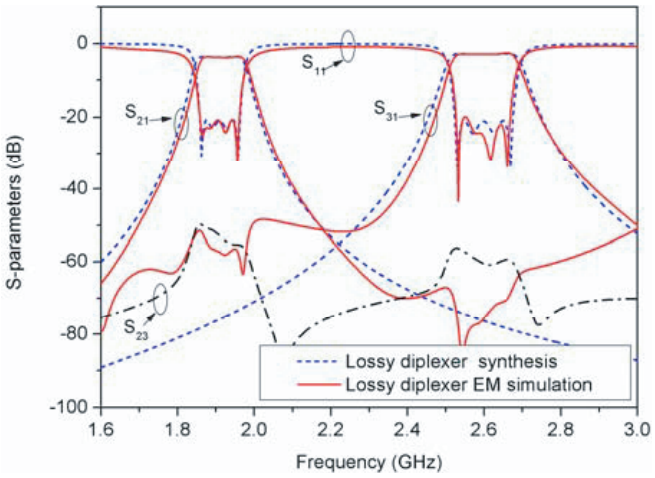

Figure 7. Lossy diplexer EM simulation results compared to theoretical results based on the coupling matrix with resistive couplings. The simulated isolation parameter (S_{23}) is shown in a black dash dot line.

The measured results of the lossy diplexer after tuning are shown in Figure 10(a) in comparison with the simulation. The return losses in both channels are better than 15 dB. The average insertion loss is 4.23 dB for the lower band and 3.43 dB for the higher band. The variation of the insertion loss over the passbands are 0.66 dB and 0.63 dB, respectively. The small deviation between the simulated and measured results is again believed to be mainly due to the tolerances of the fabrication as well as the parasitic effects from the resistors.

The comparison of the measured frequency responses between the reference diplexer and lossy diplexer is shown in Figure 10(b). The much-improved flatness of the passband from the lossy diplexer can be clearly observed from the comparison.

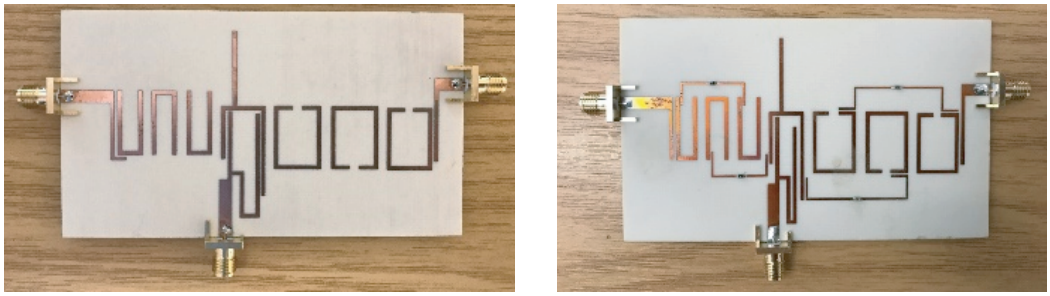

(a) (b)

Figure 8. Photographs of the fabricated reference and the lossy diplexer. (a) Reference diplexer. (b) Lossy diplexer.

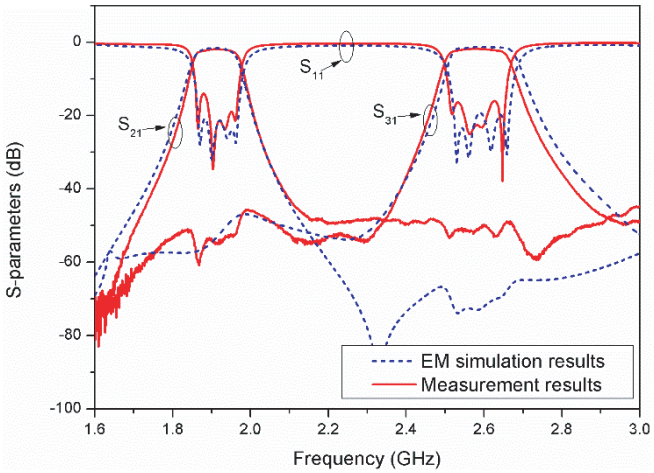

Figure 9. Measured responses of the reference diplexer in comparison with simulations.

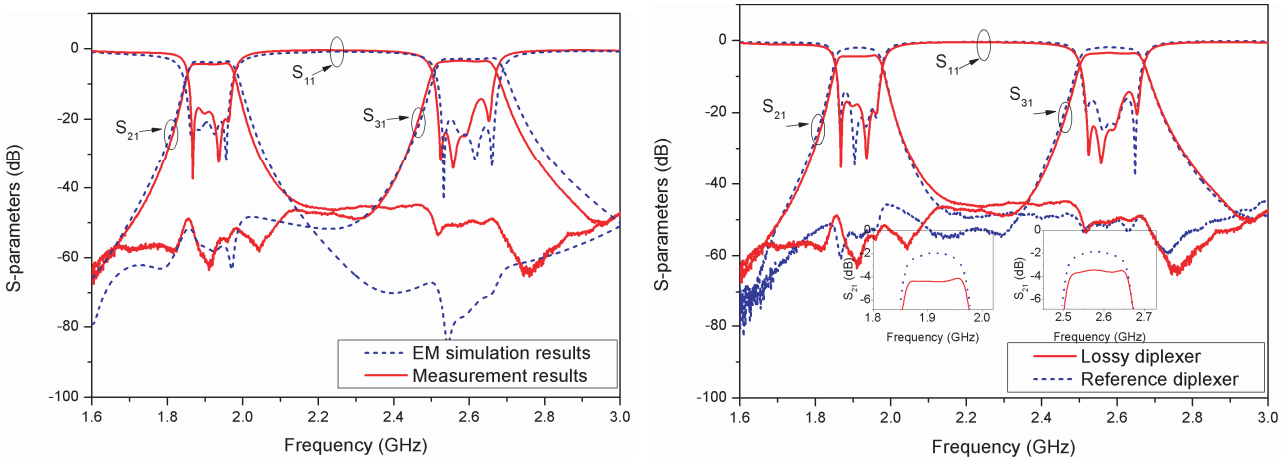

(a) (b)

Figure 10. (a) Measured lossy diplexer in comparison with simulation. (b) Measurement comparison between the lossy diplexer and reference diplexer.

5. CONCLUSION

This paper reported for the first time the extension of the lossy filter concept to a microstrip lossy diplexer. The dissipative cross couplings were used to increase the flatness of the channel passbands. A

dual-mode resonant junction with an independently controllable external coupling structure was applied to the diplexer. This enables the flexible realization of different channel bandwidths in resonator-based diplexers in a compact way, and facilitated the realization of lossy channel filters. Very good agreement has been achieved between the calculated responses from the synthesized coupling matrix, the EM simulations, and the measurement results. This has verified the synthesis method of the coupling matrix and the design approach. The flatness of the passband has been significantly improved, which is reflected by a reduction of the insertion loss variation over the two channel passbands from 1.4/1.2 dB to 0.66/0.63 dB for the low/high band. This device technology can also be used in diplexers with closer channels as well as in multiplexers. This paper focused on the demonstration of the new device function of lossy diplexer. The layout of the diplexer could be further optimized for miniaturization. A compact lossy diplexer could find applications in communication systems requiring flat channel passbands, such as in the input multiplexing block of telecommunication satellites.

REFERENCES

1. Basti, A., A. Perigaud, S. Bila, S. Verdeyme, L. Estagerie, and H. Leblond, "Design of microstrip lossy filters for receivers in satellite transponders," *IEEE Transactions on Microwave Theory and Techniques*, Vol. 62, No. 9, 2014–2024, 2014.
2. Szydlowski, L., A. Lamecki, and M. Mrozowski, "Design of microwave lossy filter based on substrate integrated waveguide (SIW)," *IEEE Microwave and Wireless Components Letters*, Vol. 21, No. 5, 249–251, 2011.
3. Basti, A., S. Bila, S. Verdeyme, A. Perigaud, L. Estagerie, and H. Leblond, "Comparison of two approaches for the design of microstrip lossy filters," *Proceedings of the 43rd European Microwave Conference*, 21–24, Nuremberg, Germany, Oct. 2013.
4. Miraftab, V. and M. Yu, "Advanced coupling matrix and admittance function synthesis techniques for dissipative microwave filters," *IEEE Transactions on Microwave Theory and Techniques*, Vol. 57, No. 10, 2429–2438, 2009.
5. Miraftab, V. and M. Yu, "Generalized lossy microwave filter coupling matrix synthesis and design," *IEEE MTT-S International Microwave Symposium Digest*, 627–630, Atlanta, GA, Jun. 2008.
6. Williams, A. E., W. G. Bush, and R. R. Bonetti, "Predistortion techniques for multicoupled resonator filters," *1984 IEEE MTT-S International Microwave Symposium Digest*, 290–291, 1984.
7. Yu, M., W.-C. Tang, A. Malarky, V. Dokas, R. Cameron, and Y. Wang, "Predistortion technique for cross-coupled filters and its application to satellite communication systems," *IEEE Transactions on Microwave Theory and Techniques*, Vol. 51, No. 12, 2505–2515, 2003.
8. Yu, M. and V. Miraftab, "Shrinking microwave filters," *IEEE Microwave Magazine*, Vol. 9, No. 5, 40–54, 2008.
9. Ni, J., W. Tang, J. Hong, and R. H. Geschke, "Design of microstrip lossy filter using an extended doublet topology," *IEEE Microwave and Wireless Components Letters*, Vol. 24, No. 5, 318–320, 2014.
10. Hunter, I., A. Guyette, and R. D. Pollard, "Passive microwave receive filter networks using low-Q resonators," *IEEE Microwave Magazine*, Vol. 6, No. 3, 46–53, 2005.
11. Qiu, L. F., L. S. Wu, W. Y. Yin, and J. F. Mao, "A flat-passband microstrip filter with nonuniform-Q dual-mode resonators," *IEEE Microwave and Wireless Components Letters*, Vol. 26, No. 3, 183–185, 2016.
12. Guyette, A., I. Hunter, and R. Pollard, "The design of microwave bandpass filters using resonators with nonuniform Q," *IEEE Transactions on Microwave Theory and Techniques*, Vol. 54, No. 11, 3914–3922, 2006.
13. Meng, M. and I. Hunter, "The design of parallel connected filter networks with non-uniform Q resonators," *2012 IEEE MTT-S International Microwave Symposium Digest*, 1–3, 2012.
14. Mateu, J., A. Padilla, C. Collado, M. Martinez-Mendoza, E. Rocas, C. Ernst, and J. M. O. Callaghan, "Synthesis of 4th order lossy filters with uniform Q distribution," *2010 IEEE MTT-S International Microwave Symposium Digest*, 568–571, 2010.

15. Gao, B., L.-S. Wu, and J.-F. Mao, "Flat-passband substrate integrated waveguide filter with resistive couplings," *Progress In Electromagnetics Research C*, Vol. 62, 1–10, 2016.
16. Shang, X. B., Y. Wang, W. Xia, and M. J. Lancaster, "Novel multiplexer topologies based on all-resonator structures," *IEEE Transactions on Microwave Theory and Techniques*, Vol. 61, No. 11, 3838–3845, 2013.
17. Chuang, M. L. and M.-T. Wu, "Microstrip diplexer design using common T-shaped resonator," *IEEE Microwave and Wireless Components Letters*, Vol. 21, No. 11, 583–585, 2011.
18. Wu, Y., Y. Wang, and L. Sun, "Independently controllable external coupling for resonant junctions in diplexers," *2018 IEEE MTT-S International Microwave Symposium Digest*, 1068–1071, 2018.
19. Hong, J. S. and M. J. Lancaster, *Microstrip Filters for RF/Microwave Applications*, Wiley, New York, NY, USA, 2001.
20. Miraftab, V. and M. Yu, "Generalized lossy microwave filter coupling synthesis and design using mixed technologies," *IEEE Transactions on Microwave Theory and Techniques*, Vol. 56, No. 12, 3016–3027, 2008.
21. Zhang, X. Y., J. X. Chen, Q. Xue, and S. M. Li, "Dual-band bandpass filters using stub-loaded resonators," *IEEE Microwave and Wireless Components Letters*, Vol. 17, No. 8, 583–585, 2007.
22. "HFSS high frequency structure simulator," USA, [Online]. Available: www. ansys. com.